ACS APPLIED POLYMER MATERIALS

pubs.acs.org/acsapm Article

Light-Activated Antibacterial Polymeric Surface Based on Porphycene

Edwin J. Gonzalez Lopez, Melisa Renfige Rodriguez, Sofia C. Santamarina, Lorena Macor, Luis A. Otero, Miguel A. Gervaldo, Andrés M. Durantini, Edgardo N. Durantini, Javier E. Durantini,* and Daniel A. Heredia*

Cite This: *ACS Appl. Polym. Mater.* 2023, 5, 943−956 Read Online

ACCESS | Metrics & More | Article Recommendations | Supporting Information

ABSTRACT: A photoactivatable antimicrobial polymeric surface based on a porphycene derivate was efficiently prepared and evaluated to kill pathogenic microorganisms. The development of this self-sterilizing material consisted in the electrochemical polymerization of a peripherally tetra-substituted porphycene bearing benzyl-carbazole groups (**Pc-Cbz**). The latter were used as electropolymerizable centers, while the porphycene core triggered the photodynamic action. The electrodeposited photodynamic films (**P-Pc-Cbz**) were obtained in a reproducible and controllable manner. Electrochemistry studies combined with spectroscopic measurements demonstrated that the porphycene core remains unaffected after the electrodeposition process. Moreover, it retains its spectroscopic and photodynamic properties within the polymeric matrix. The photoactive layers were photostable and able to produce reactive oxygen species (ROS) by both photodynamic mechanisms. Also, the antimicrobial efficiency of **P-Pc-Cbz** was evaluated against two antibiotic-resistant strains (methicillin-resistant *Staphylococcus aureus* and *Escherichia coli*), exhibiting an antimicrobial action higher than 99.998% over these Gram-positive and Gram-negative bacteria. This work represents the first electropolymerization of a porphycene derivative and the first porphycene-based photobiocidal surface. **P-Pc-Cbz** shows great potential as an efficient self-sterilizing coating activated by visible light.

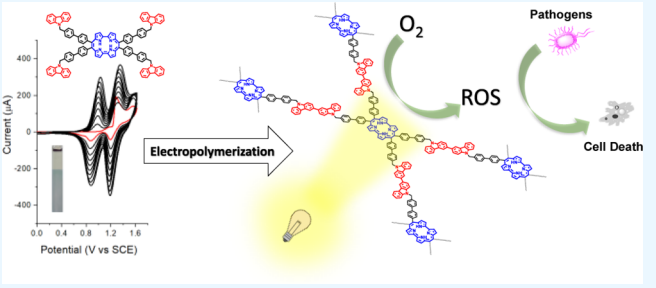

KEYWORDS: *porphycene, antimicrobial, photodynamic inactivation, electropolymerization, carbazole, self-sterilizing surface, light-activated polymer*

1. INTRODUCTION

Bacterial infections generated by clinically resistant strains have become global threats to human health and environmental safety.[1,2] In fact, it is a severe problem that generates relevant human and economic losses. The rise of antimicrobial resistance by microorganisms is expected to be responsible for the major causes of death worldwide in the near future.[3] In this scenario, considering that surfaces are the most significant reservoirs of pathogenic microorganisms, there is a need to improve and develop self-sterilizing and antimicrobial surfaces.[4−6]

Aiming to reduce bacterial resistance spread, photodynamic inactivation (PDI) of microorganisms has emerged as a promising strategy to assist in the current antibiotic crisis.[7−9] This therapy combines molecular oxygen and a photosensitizer (PS) that generates reactive oxygen species (ROS) after being activated by light.[10] These ROS react with a wide range of biomacromolecules and organelles of the microbial cell, producing irreversible damage that leads to the microorganisms' death.[10] Thus, the immobilization of different PSs on solids surfaces is a plausible technology that can be used to fabricate sanitized and antimicrobial coatings, addressing the needs mentioned above .[4,7,8]

An interesting approach to attach PSs to different surfaces is the electrochemical polymerization of suitable designed electroactive monomers. In this frame, the organic polymeric thin films obtained through electrodeposition are a class of potential materials for preparing highly efficient surfaces able to generate ROS.[11−15] The use of electrochemical polymerization has the advantage that the material and the deposition as a thin film is obtained in the same step under mild conditions, covering the entire surface with the desired shape. Furthermore, the electrodeposition can be performed with fine control over the film characteristics, such as roughness and

Received: October 29, 2022
Accepted: December 14, 2022
Published: January 3, 2023

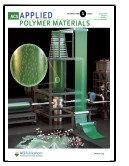

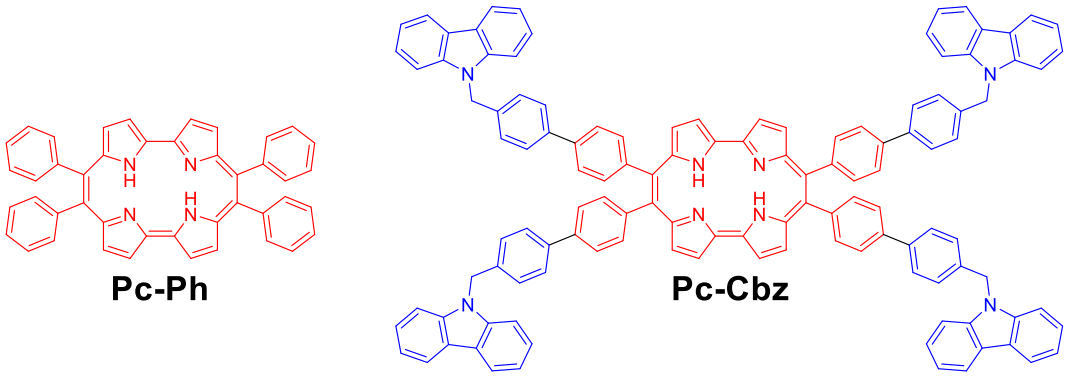

Figure 1. Molecular structures of porphycenes **Pc-Ph** and **Pc-Cbz**.

thickness, two essential parameters in the fabrication of functional coatings.[16,17]

Our group has recently shown that electrodeposited films of dendrimeric porphyrins, bearing carbazole groups as electropolymerization centers, exhibited potential applications as self-disinfecting surfaces.[12] PDI treatments demonstrated the efficiency of these polymers to photokill Gram-positive and Gram-negative microorganisms after visible light illumination. In addition, Comuzzi and co-workers informed the electrosynthesis of photoactive surfaces using dipyrromethanes as monomers and imprinting a pentaphyrin compound as a PS.[18] These thin organic films were also able to inactivate *Staphylococcus aureus* suspensions. Moreover, Ballatore et al. have also proved that a *meso*-substituted porphyrin monomer containing four carbazole units could generate electrodeposited polymers with interesting antimicrobial activity.[19]

Notwithstanding porphyrins are the most common and widely studied tetrapyrrolic compounds; they present relatively low absorption in the red visible region. Therefore, there is an increasing interest in developing and applying constitutional isomers of porphyrins with high red absorption, such as the porphycene derivatives. These macrocycles formed by two α,α'-bipyrrole moieties linked by two ethylene bridges[20] were first reported by Vogel et al.[21] Porphycenes possess distinguished photochemical properties, such as stronger red absorption and higher photostability in comparison with porphyrins.[22−25] They also have relatively high fluorescence quantum yield and efficient singlet oxygen ($^1O_2$) generation.[22,26,27] These properties stimulated the design and synthesis of hundreds of porphycene-based compounds applied mainly in photodynamic therapy.[20,28,29]

Even though that porphycenes possess the mentioned advantages over porphyrins,[22−25,28] few works have been reported using compounds based on the porphycene structure for PDI.[30−33] Furthermore, there are even fewer studies focusing on incorporating these constitutional isomers into polymeric materials. Ono et al. recently reported the synthesis of a *meso*-tetraalkylporphycene bearing reactive sites and the formation of porphycene-polydimethylsiloxane hybrid films with remarkable photophysical properties.[34] Abe et al. informed the oxidative electrochemical polymerization of an axially bound bithiophene-pyridine complex of ruthenium(III)-porphycene and the formation of a polymeric film on indium tin oxide (ITO) electrodes.[35] This limited number of investigations of porphycenes in comparison with porphyrins[36] could be understood due to their complex, expensive, and ineffective synthetic sequences.[20] Nevertheless, Ravikanth and Hisaeda and co-workers have improved the procedures to synthesize *meso*-arylporphycenes at gram scale.[37,38] Thus, in view of the advantages of porphycene as PSs, the possibility that offers the new synthetic process, and the mentioned versatility of electrochemical deposition technique, we explored the development of a photoactivable antimicrobial surface based on an electrodeposited polymer of porphycene. We hypothesize that the electrosynthesis of a porphycene-based polymer will produce ROS upon photoexcitation, inactivating pathogenic microbes.

In this study, we report the development of antibacterial photodynamic coatings obtained from the electropolymerization of a suitably functionalized porphycene. The electroactive monomer based on a carbazole *meso*-tetrasubstituted porphycene (**Pc-Cbz**, Figure 1) was characterized and compared with its noncarbazole analog (**Pc-Ph**, Figure 1) using cyclic voltammetry (CV) and differential pulse voltammetry (DPV) methods. The electrochemically generated carbazole radical cation in each *meso* position of **Pc-Cbz** underwent the well-known dimerization coupling to produce a hyperbranched polymeric structure (**P-Pc-Cbz**).[17,39] Spectroscopic, electrochemical, and photoelectrochemical characterization demonstrated that the tetrapyrrolic macrocyclic ring remains unaltered after the polymerization procedure, allowing the preparation of this first example of a carbazole-porphycene polymeric film. The photosensitizing action of **P-Pc-Cbz** to produce $^1O_2$ was investigated and compared with the **Pc-Cbz** monomer. The capability to photogenerate $O_2^{\cdot-}$ was also evaluated. Microbiological testing of the antibacterial coating using Gram-positive (methicillin-resistant *S. aureus*, MRSA) and Gram-negative bacteria (*Escherichia coli* EC7, resistant to β-lactam antibiotics) was carried out to evaluate its bactericidal activity against these antibiotic-resistant pathogens. Our outcomes showed that this self-sterilizing and light-activated antimicrobial polymer is potentially helpful to conserve aseptic environments and control the transmission of pathogens, limiting the risk of cross-contamination. As far as we know, this work represents the first application of a porphycene-based polymeric surface in the photoinactivation of pathogenic microorganisms.

2. EXPERIMENTAL SECTION

2.1. Electrochemistry and Electrodeposition. The reference (**Pc-Ph**) and the electropolymerizable monomer (**Pc-Cbz**) were synthesized as previously reported.[33] 1,2-Dichloroethane (DCE) was purified by distillation with CaH_2 (50 g/L) as a water removal agent. The ITO-coated glass substrates (Delta Technologies, nominal resistance 8−12 Ω/ square) were cleaned in an ultrasonic bath with

https://doi.org/10.1021/acsapm.2c01890
ACS Appl. Polym. Mater. 2023, 5, 943−956

acetone-isopropyl alcohol (1:1), ethanol, and deionized water, and subsequently dried with nitrogen.

Electrochemical studies (CV and DPV) were performed with a potentiostat-galvanostat PalmSens4 using a three-electrode cell configuration with a Pt working electrode, a large area Pt counter electrode, and an Ag wire pseudoreference electrode. In the electrochemical characterization of **Pc-Ph** and **PC-Cbz**, concentrations of around 0.5×10^{-3} M were used. **Pc-Ph** and **Pc-Cbz** were dissolved in DCE containing 0.10 M tetrabutylammonium hexafluorophosphate ($TBAPF_6$) as supporting electrolyte. Before each electrochemical characterization, the solutions of **Pc-Ph** and **Pc-Cbz** were deoxygenated by argon bubbling. **P-Pc-Cbz** polymeric films were generated by 10 continuous voltammetric cycles in the 0.0−1.6 V range. The electrochemical responses of the electropolymerized films were carried out in the same deoxygenated electrolyte solution. In all the electrochemical measurements, the Pt working electrode was mechanically cleaned between experiments by polishing with alumina paste (0.3 μm) followed by solvent rinses. After each voltammetric experiment, ferrocene was added as an internal standard and the potential axis was calibrated against the formal potential for the saturated calomel electrode (SCE). The experimental conditions used in the generation of films over ITO electrodes were identical to those used for Pt electrode. The **P-Pc-Cbz** film thickness was ∼70 nm. These values were estimated following the methodology reported by Zhang et al.[40] where it is supposed that after electropolymerization, the change in the absorption coefficient of the porphycene chromophore was negligible.

2.2. Scanning Electron Microscopy. **P-Pc-Cbz** polymeric films deposited on the ITO electrode were coated with a thin chromium layer (∼3 nm) via sputtering to improve the conductivity. Then, the surfaces were examined using a scanning electron microscope (SEM). SEM images were obtained using a field emission SEM (FE-SEM), Sigma Zeiss (LAMARX facilities). An ITO electrode without electrodeposited polymer was also analyzed for comparative purposes.

2.3. Atomic Force Microscopy (AFM). AFM experiments were performed using an Agilent 5500 SPM microscope (Agilent Technologies, Inc.) working in acoustic AC mode. Commercial silicon cantilever probes with aluminum backside coating and nominal tip radius of 10 nm (MikroMasch, NSC15/Al BS/15, spring constant ranging 20−75 N m^{-1}) were employed just under their fundamental resonance frequencies of about 325 kHz.

2.4. Spectroscopic and Spectroelectrochemical Studies. Absorption spectra of **Pc-Cbz** and **P-Pc-Cbz** were acquired in diluted DCE solution and in thin films, respectively. The measurements were carried out at room temperature in a quartz cuvette (1 cm path length) for **Pc-Cbz**, while **P-Pc-Cbz** films were placed in the spectrometer cell holder. An ITO electrode without polymer was used as background correction.

Spectroelectrochemical experiments were carried out in a custom cell manufactured from a commercial UV−vis cuvette. **P-Pc-Cbz** films on ITO, Pt, and an Ag wire were used as working, counter, and pseudo-reference electrodes, respectively. The cell was placed in the optical path of the sample light beam. The background correction was obtained by taking a UV−vis spectrum of a blank cell (an electrochemical cell with an ITO working electrode without the film) with identical conditions to those used for the polymer film experiments. During the measurements, spectra were taken as a function of time under kinetic control.

2.5. Detection of $^1O_2$. The production of $^1O_2$ photosensitized by **P-Pc-Cbz** was assessed by the photooxidation of 1,3-diphenylisobenzofuran (DPBF). **P-Pc-Cbz** surface (0.7 × 2.5 cm) was dipped in an air-equilibrated solution of DPBF in *N*,*N*-dimethylformamide (DMF), and it was then irradiated with light (wavelength range: 455−800 nm, 30 mW/cm^2).[11,12] A solution containing **Pc-Cbz** and DPBF was also irradiated under the same conditions to conduct comparative studies. The kinetic of photodecomposition of DPBF was examined by following the decrease of its absorption band at λ_{max} = 414 nm as a function of the irradiation time. The slopes obtained from the linear fit of the $\ln(A_0/A)$ vs time represent the observed rate constants (k_{obs}).[33]

2.6. Detection of Superoxide Radical Anion. The photogeneration of superoxide radical anion ($O_2^{\cdot-}$) was determined by the nitro blue tetrazolium (NBT) method. To assess the reduction of NBT, the **P-Pc-Cbz** surface was dipped in a solution containing 0.2 mM NBT and 0.5 mM reduced nicotinamide adenine dinucleotide (NADH). Then it was irradiated with light (455−800 nm, 30 mW/cm^2) in aerobiosis. The diformazan production (NBT reduction product) was monitored by the increase of its absorbance band at λ_{max} = 560 nm.[11,12] Also, a solution containing NBT and NADH was irradiated as a control experiment.

2.7. Photobleaching. Photobleaching of **P-Pc-Cbz** surfaces was evaluated by following the decrease of the absorbance at λ_{max} = 393 nm (Soret band). The **P-Pc-Cbz** film was placed in a quartz cell (optical length: 1 cm) containing air-equilibrated phosphate-buffered saline (PBS, pH = 7) solution. It was then irradiated with visible light under the same conditions described below for PDI experiments. Absorption spectra were acquired at regular time intervals. The observed rate constant of photobleaching (k_{obs}^P) determined from the slope of the linear fit of the semilogarithmic plot ln (A_0/A) vs irradiation time was used to calculate the half-life time of photobleaching ($\tau_{1/2}^P$) as indicated in eq S1.[11,12]

2.8. PDI Treatments. MRSA ATCC 43300 and *E. coli* EC7 were used in PDI treatments. These bacteria were previously identified and characterized.[41] Preparation of cultures to afford ∼10^5 colony-forming units (CFU)/mL in PBS was achieved as reported in the Supporting Information.[42]

For the heterogeneous (solid−liquid) PDI treatments mediated by the polymeric surfaces, cell suspensions of MRSA and *E. coli* in PBS (200 μL, ∼10^5 CFU/mL) were transferred to 96-well microtiter plates. Then, two square surfaces of **P-Pc-Cbz** (0.3 × 0.3 = 0.09 cm^2) were added to the wells. The system was irradiated with visible light (350−800 nm, 90 mW/cm^2) for 30 and 60 min. After treatment, the viability of MRSA and *E. coli* was determined by serial 10-fold dilutions (PBS) and plated on tryptic soy broth (TSA) to count CFU. Each suspension was plated in triplicate. The plates were incubated for 24 h at 37 °C in the dark, and the number of CFU was counted. Irradiated controls (60 min) were carried out with cultures without surfaces and with an ITO electrode. Also, dark controls (60 min) using **P-Pc-Cbz** and ITO were performed. For recycling experiments, after each photoinactivation treatment, the wells and the surfaces were washed and cleaned with PBS. Then they were reutilized in two more experiments. All experiments were repeated separately three times.

3. RESULTS AND DISCUSSION

3.1. Molecular Structures. Two structurally related porphycenes with different substitution patterns at the *meso* position were studied to develop a novel photoactivable material (Figure 1). Both PSs were synthesized by us as previously described.[33] First, molecular structure of **Pc-Ph** possesses four phenyl rings around the porphycene core, while **Pc-Cbz** has four benzyl-carbazole moieties on the periphery of the macrocycle. **Pc-Cbz** is a combination of **Pc-Ph** with peripheral polymerizable carbazole groups. **Pc-Ph** molecule was used as a reference and model compound to compare and facilitate the data interpretation. **Pc-Cbz**, the electropolymerizable monomer, has a methylene group between each carbazole and phenyl moiety that avoid the conjugation with the porphycene core, allowing the individual electrochemical behavior of these polymerizable units. Thus, the carbazole centers can be used to generate polymeric surfaces containing photoactive cores of porphycene that can trigger the photodynamic antimicrobial action.

The polymeric films obtained by the electropolymerization of **Pc-Cbz** should generate an effective photocytotoxic effect against microorganisms due to the capability of the tetrapyrrolic macrocycle to produce ROS after its irradiation with visible light. Therefore, electrogenerated films deposited

https://doi.org/10.1021/acsapm.2c01890
ACS Appl. Polym. Mater. 2023, 5, 943−956

on ITO surfaces would prove a promising self-sterilizing coating with plausible applications in the photoinactivation of microbial cells. Finally, it is worth highlighting that the insolubility of porphycene in aqueous media is a disadvantage for homogenous PDI. Nevertheless, this is an advantage for heterogenous PDI since it ensures higher stability avoiding the loss of PS by leaching in aqueous environments.

3.2. Electrochemical Characterization of the Monomers. Electrochemical studies of **Pc-Cbz** and **Pc-Ph** were performed to obtain detailed information about the redox processes. **Pc-Ph** was used as a model compound to facilitate the peak assignments. Figure 2 shows the electrochemical properties of both monomers characterized using CV in a conventional three-electrode electrochemical cell at room temperature in DCE using a Pt working electrode. The oxidation and reduction potential values for both tetrapyrrolic macrocycles are gathered in Table S1.

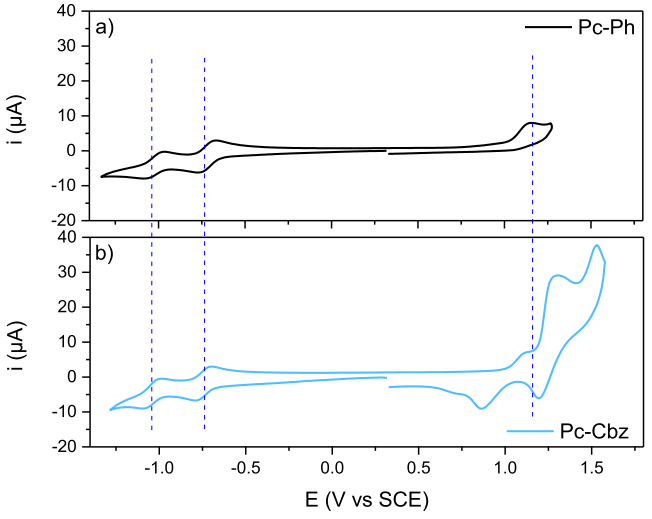

Figure 2. Cyclic voltammograms of (a) **Pc-Ph** and (b) **Pc-Cbz** in DCE containing 0.10 M $TBAPF_6$. Pt working electrode, scan rate 100 mV/s.

Pc-Ph presents two quasi-reversible reduction waves at −0.73 and −1.03 V and an irreversible oxidation wave at 1.16 V that could be assigned to the formation of the radical anion, dianion, and radical cation of the porphycene ring, respectively (Figure 2a).[37,43,44] These results are in full agreement with the previously reported results for *meso*-substituted tetra-arylated porphycenes.[37,38,43,44] **Pc-Cbz** also presents two quasi-reversible one-electron reduction processes at −0.76 and −1.06 V, but in the anodic scan, three oxidation peaks at 1.15, 1.31, and 1.53 V are detected (Figure 2b). These oxidation processes are not totally reversible, and the complementary reduction peaks are absent or present complex electrochemistry.

DPV measurements usually allow better peak discrimination in multielectronic electrochemical processes. As observed in Figure S1, DPV potential peaks are in concordance with the CV studies. **Pc-Ph** shows one oxidation peak, while **Pc-Cbz** exhibits three oxidation waves. Also, both molecules present two reduction peaks at similar potential values.

According to the CV and DPV studies and comparing both molecules, it is possible to assign the first oxidation peak to the formation of porphycene macrocycle radical cation in both cases. On the other hand, the second and third oxidation peaks observed in **Pc-Cbz** are attributed to the complex electrochemical-chemical-electrochemical (ECE) processes typically observed in carbazole-containing derivatives.[45] The carbazole radical cations formation leads to the coupling of two of these species generating dicarbazole (**DCbz**), whose first oxidation process occurs at a lower potential.[46] Also, at the applied potential corresponding to the second oxidation peak, **DCbz** dication can be generated. All these processes are affected by the proximity of oxidizable carbazole groups.[45]

3.3. Electrosynthesis of Polymeric Films. Once the redox processes of **Pc-Cbz** were known and assigned,

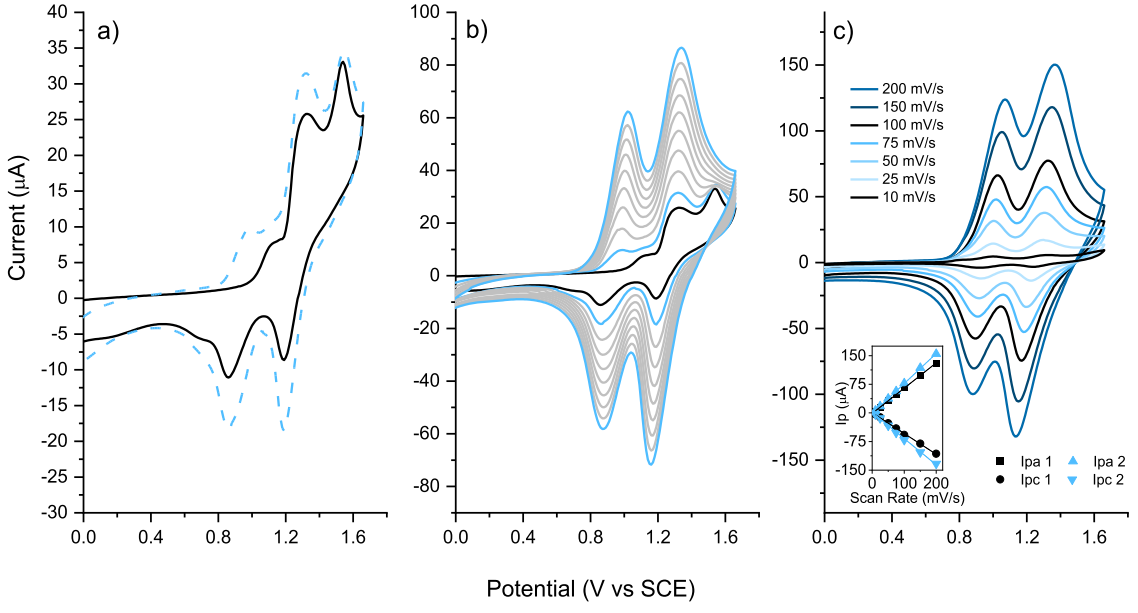

Figure 3. (a) First (solid line) and second (dotted line) anodic sweep of **Pc-Cbz**, scan rate 100 mV/s. (b) Ten consecutives cyclic voltammetric scans of **Pc-Cbz**, scan rate 100 mV/s. (c) Voltammetric responses of **P-Pc-Cbz** over Pt electrode at different scan rates. Inset: anodic and cathodic peak currents vs scan rate of **P-Pc-Cbz**. All measurements were conducted using a Pt electrode in DCE containing 0.10 M $TBAPF_6$.

https://doi.org/10.1021/acsapm.2c01890
ACS Appl. Polym. Mater. 2023, 5, 943−956

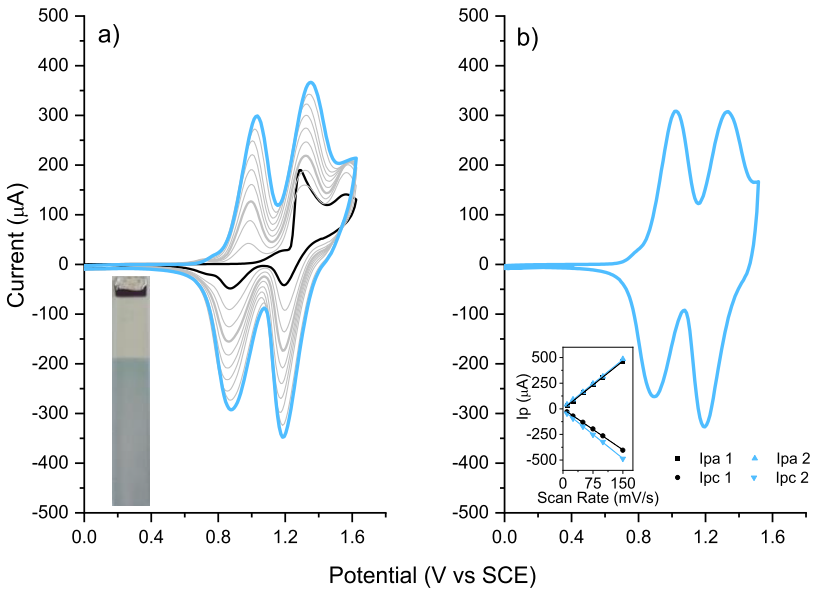

Figure 4. (a) Ten consecutive cyclic voltammetric scans of **Pc-Cbz** on ITO electrode, scan rate 100 mV/s. Inset: photographic imagen of the **P-Pc-Cbz** electropolymerized film. (b) Voltammetric response of **P-Pc-Cbz** on ITO electrode, scan rate 100 mV/s. Inset: anodic and cathodic peak currents vs scan rate for **P-Pc-Cbz** on ITO electrode. All measurements were conducted in DCE (0.10 M $TBAPF_6$).

polymeric films were electrosynthesized using CV. As mentioned before, in the first anodic scan of **Pc-Cbz** (from 0.00 to 1.65 V), three irreversible peaks were observed. In the second anodic scan (Figure 3a), a new oxidation process and also increases in the oxidation currents at slightly lower potentials than the second and third oxidation waves can be seen. The formation of new peaks after the first anodic scan indicates that the generated radical cations are involved in an ECE reaction generating a product that is oxidized easier than the monomer.[47,48] After 10 continuous cycling in the same potential range, **Pc-Cbz** showed progressive increases in the oxidation and reduction currents (Figure 3b), which is indicative of the presence of a coupling reaction and the formation of an electroactive film on the electrode surface. On the other hand, cycling of **Pc-Ph** in the same potential window does not evidence any increase in oxidation/reduction currents due to the absence of electropolymerizable **Cbz** moieties.

To confirm the presence of an electroactive species on the surface of the working electrode, this was carefully removed from the electrochemical cell, rinsed with DCE, and placed in a porphycene-free solution containing only supporting electrolyte. Figure 3c shows the redox response of **Pc-Cbz** film (**P-Pc-Cbz**) at different scan rates. The observed electrochemical responses confirm the deposition of an electroactive product on the electrode surface, which could be generated by coupling of two carbazole moieties.[47,48] **P-Pc-Cbz** presents an anodic electrochemical response characterized by two well-defined bell shape oxidation peaks at 0.97 and 1.31 V (Figure 3c). Moreover, the anodic and cathodic peak currents for both couples show a linear relationship with the scan rate (inset Figure 3c), which is characteristic of a product irreversibly adsorbed on the electrode surface.[48] Additionally, a comparable effect was observed (Figure S2a,b) when the electropolymer was grown cycling to the second oxidation wave of **Pc-Cbz** (1.45 V vs SCE instead 1.65 V as in the former case). As can be seen in Figure S2a, increases in the oxidation/reduction currents were also detected. Correspondingly, the electrochemical response of the film presented two redox systems with peak currents proportional to the scan rate (Figure S2b). On the contrary, Figure S2c shows that no oxidation/reduction current increases were detected when the first peak was repeatedly cycled (applied potential until 1.2 V vs SCE). This is a logical result since this first process corresponds to the formation of the radical cation of the porphycene macrocycle.

It is known that the oxidation of carbazole groups generates unstable radical cations, which undergo a dimerization reaction to form **DCbz** units (Scheme S1). Consequently, electrochemical oxidative cycling of molecules containing two or more carbazole groups usually produces polymers on conductive substrates.[12,17] **Pc-Cbz** has four carbazole groups linked to the macrocycle, each one with two positions available to dimerize (positions 3 and 6). Therefore, during the continuous anodic cycling of the monomer, the carbazole units undergo a dimerization process that leads to the growth of a polymeric film on the Pt electrode.

Furthermore, the electrochemical response of **P-Pc-Cbz** is attributed to the generation and permanence of a polymeric film containing **DCbz** units as building blocks over the electrode surface. The electropolymers containing **DCbz** residues commonly present two reversible oxidation peaks (as observed in the **P-Pc-Cbz** redox responses), which are associated with the formation of the radical cation and the dication of **DCbz** units.[45,49] On the other hand, *meso*-tetraphenyl porphycenes generally present one oxidation related to the formation of the radical cation.[37,43,44] In this sense, **P-Pc-Cbz** polymer is formed by porphycene centers connected one to the other by **DCbz** units (Figure S3). This leads to the formation of a complex three-dimensional polymer network in which tetrapyrrolic macrocycles are embedded in the polymer matrix. Figure S3 also shows the idealized structure obtained from geometric optimization through molecular mechanic calculations for five units of the monomer. It is possible to observe the formation of the **DCbz** units produced by the coupling of the electrochemically generated carbazole radical cations. Furthermore, it is also possible to

https://doi.org/10.1021/acsapm.2c01890
ACS Appl. Polym. Mater. 2023, 5, 943−956

perceive the ramifications of the polymeric structure generating a three-dimensional dendrimeric type structure.

3.4. Fabrication of Antimicrobial Polymeric Surfaces. With the aim to study the antimicrobial properties of the polymeric materials, **P-Pc-Cbz** films were generated over semitransparent ITO electrodes. Figure 4a shows 10 repetitive cyclic voltammograms of **Pc-Cbz** using an ITO working electrode. A growth of the oxidation/reduction currents with each new cycle can also be observed. The electrochemical response of **P-Pc-Cbz** in DCE depicts two redox processes (Figure 4b) that are very similar to those obtained using the Pt electrode. Additionally, a linear ratio between the oxidation/reduction peak currents and the scan rate is observed in the inset of Figure 4b. These results confirm that **Pc-Cbz** can also be deposited over ITO electrodes.

3.5. Spectroscopic Properties. The absorption characteristics of **P-Pc-Cbz** deposited on ITO electrode were determined by UV−vis spectroscopy and were compared with the repetitive unit **Pc-Cbz**. Figure 5 shows the absorption

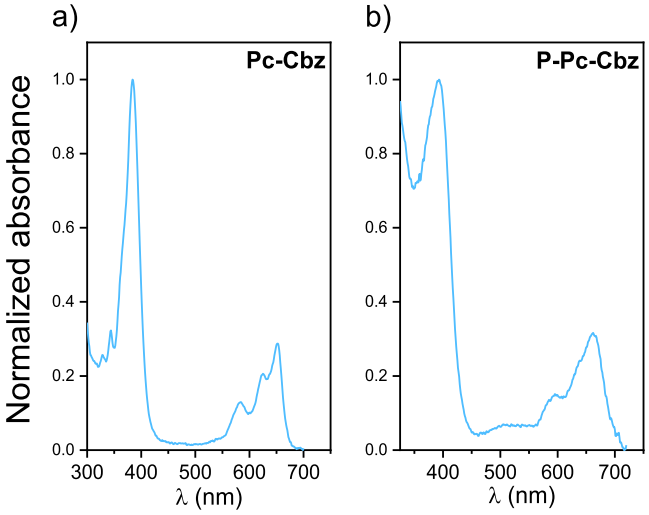

Figure 5. Absorption spectra of (a) **Pc-Cbz** in DCE and (b) **P-Pc-Cbz** deposited on ITO electrode.

spectra of **Pc-Cbz** in DCE and the electrodeposited **P-Pc-Cbz** on ITO. The main spectroscopic properties are grafted in Table S2. The monomer presents the strong absorption of the Soret band in the blue region (λ_{max} = 384 nm) and the characteristic Q bands in the red region of the electromagnetic spectrum (between 500 and 700 nm).[22,37] The high red absorption of **Pc-Cbz** compared with related porphyrins (typical extinction coefficient ~10^4 and ~10^3 for porphyrin) permits the use of lower light doses to produce a comparable concentration of excited states.[22,28] On the other hand, the absorption spectrum of **Pc-Cbz** (Figure 5a) is essentially the addition of the spectra of **Pc-Ph** and phenyl-carbazol moieties, which indicates the lack of interaction of the two units in the ground state. The electronic transitions corresponding to the absorption of carbazole moieties can be observed in the UV region (between 300 and 350 nm).[12,33]

Regarding the polymer **P-Pc-Cbz**, the absorption spectrum exhibits similar spectroscopic behavior to the monomer, retaining the spectroscopic properties of the porphycene-based chromophore (Figure 5b). The Soret and Q bands are well defined despite the fact that the solid state is an extensively aggregated system. However, these electronic transitions corresponding to the porphycene core are slightly broadened and red-shifted by approximately ~9 nm compared to **Pc-Cbz** in solution. These outcomes suggest a weak interaction among the porphycene cores embedded in the polymeric matrix. In addition, an additional characteristic of this polymeric system is that the **DCbz** units could act as a light-harvesting donor and transfer the energy to the porphycene core, improving ROS photogeneration and, consequently, the antibacterial performance.[12,50−52]

Finally, spectroscopic studies not only confirm the presence of the tetrapyrrolic nucleus in the polymer structure after the electrodeposition but also demonstrate that the electrochemical polymerization process does not alter the structure of the macrocycle.

3.6. Spectroelectrochemical Characterization of P-Pc-Cbz. Spectroelectrochemical studies of **P-Pc-Cbz** on ITO electrode were performed in order to support that **DCbz** centers are present as cross-linkers in the polymer molecular structure. Absorption spectra of the polymeric films were taken at different applied potentials. The one obtained at neutral state (0.00 V) was subtracted from each individual spectrum, and then the resulting spectra were plotted as ΔAbs (Figure 6).

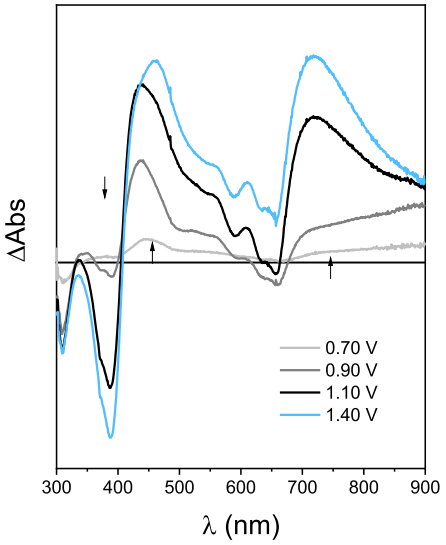

Figure 6. Difference absorption spectra of **P-Pc-Cbz** deposited on ITO electrodes. Anodic scan, DCE, 0.10 M $TBAPF_6$.

Positive absorptions correspond to the formation of a new light-absorbing species, and negative absorptions are due to species bleached in the oxidation process. At the foot of the first oxidation wave (0.70 V), a band at 440 nm and another one that extends from 700 nm to the IR region appear. At more anodic potentials (0.90 V), these two bands are increased and, at the same time, the bleaching of the Soret and Q bands can be seen, indicating that the porphycene macrocycle is oxidized. When the applied potential reaches the first oxidation peak (1.10 V), a new broad band develops with a maximum at around 720 nm, while the band at 440 nm and the bleaching of the Soret band continue increasing in intensity. At 1.40 V (film fully oxidized), all the last-mentioned bands reach their maximum values.

Thus, the electrochemical and spectroelectrochemical studies are in agreement with the presence of porphycene and **DCbz** units in the polymeric structure of **P-Pc-Cbz**. Oxidation of the film produces **DCbz** radical cations, which

https://doi.org/10.1021/acsapm.2c01890
ACS Appl. Polym. Mater. 2023, 5, 943−956

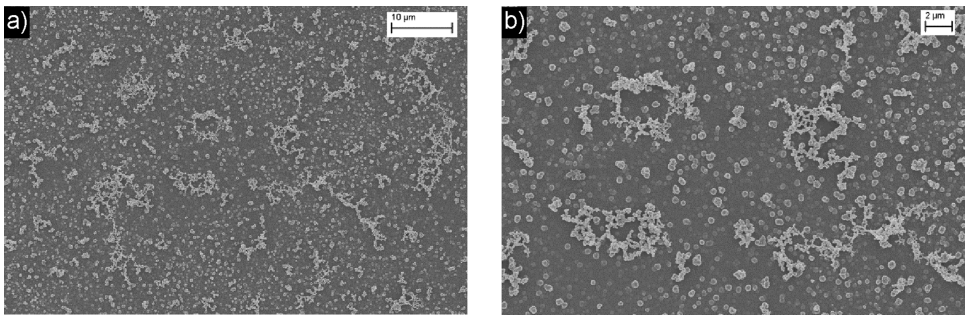

Figure 7. SEM images of **P-Pc-Cbz** films with different magnification deposited over ITO substrate (a) 1500× and (b) 3500×.

commonly present two bands: one at around 400 nm and a second one that starts at 700 nm and extends to the IR zone.[12,17,45,49] When the film is more oxidized the bleaching of the Soret and Q bands is detected, indicating the oxidation of the macrocycle. At more anodic potentials applied, the apparition of the new band at 720 nm and the increase of the band at 420 nm are attributed to the formation of **DCbz** dication and porphycene radical cation.[53,54] Therefore, the spectroelectrochemical experiment supports a polymeric chemical structure where the porphycene cores are connected by **DCbz** units. Moreover, a complementary experiment in the regime of negative applied potentials was also performed. Absorption spectra of **P-Pc-Cbz** were taken between 0.00 and −2.00 V (see Figure S4). The difference spectrum of **P-Pc-Cbz** at an applied potential of −1.10 V displays two negative absorptions at 400 and 650 nm and three positive bands: one at 380 nm, an absorption wave in the visible region, and lastly a broadband that extends to the near-infrared. It is clearly observed that as the applied potential increases (from −1.10 to −2.00 V), the absorption of the bands at around 400 and 650 nm decreases markedly. Concomitantly, the absorption of the broadband in the near-infrared (range from 750 to 1000 nm) and in the near-ultraviolet (region below 380 nm) continues growing. Four isosbestic points are clearly denoted at 375, 420, 570, and 690 nm, indubitably showing the bleaching of the porphycene Soret and Q bands. The latter confirms that the new species created by applying an electrical potential was generated from the transformation of the original material (i.e., the neutral porphycene). The spectroelectrochemical data fully agree with the formation of the porphycene radical anion during the cathodic voltammetric cycle of **P-Pc-Cbz**. Similar results were previously reported, in which the transient absorption spectrum of the π radical anion of tetraphenylporphycenes was obtained by photoinduced electron transfer from tetramethyl-phenylenediamine to the triplet state of the porphycenes in benzonitrile.[53] Furthermore, analogous bands were also observed for the π radical anion of unsubstituted and tetraalkylporphycenes.[22,55] These results also demonstrate that the porphycene nucleus remained in the polymer after the electrochemical polymerization process.

3.7. Morphological Properties of P-Pc-Cbz. The morphology of organic polymeric films is an essential parameter when they are planned to be used as functional materials. Usually, the active area involved in superficial chemical and/or physical processes depends not only on the chemical structure of the material but also on the morphological properties of the surface, which is strongly influenced by the film synthesis and deposition procedures, especially when electrochemical synthesis is used.[16,56] Furthermore, the existence of cracks or pinholes on the surface can induce physicochemical processes that affect the performance and reproducibility of the materials under study and development. The surface morphology of the **P-Pc-Cbz** films was analyzed by SEM, and the obtained images are shown in Figure 7a,b. As can be observed in Figure 7a, the complete coverage of the ITO surface by the polymeric film without large grains, islands, cracks, or pinholes could be achieved after the electrodeposition process. The surface is highly rough in comparison with the bare ITO (see Figure S5) and some structures compatible with polymeric dendrites emerging from the surface are detected, which are more evident in Figure 7b. These fused agglomerations were observed by us in the cases of other structural related electropolymers and were associated with the dendrimeric nature of the constituent monomers.[12,56]

The surface morphologies of the obtained polymer films were also examined with AFM. Figure S6 shows a typical acoustic AC mode AFM height mode image from the electrodeposited film of **P-Pc-Cbz** on ITO. As it was previously reported for structurally related electrogenerated polymers, globular-like microstructures are observed in the analyzed films.[57] The observed microstructure must be a consequence of the nucleation and further growing process itself and not just a homogeneous decoration of the ITO surface. This conclusion is confirmed by comparing the average surface RMS roughness measured over an area of 5.5 × 5.5 μm for the electrodeposited films, being 4.75 nm a much rougher surface than the ITO (1.32 nm).[57]

3.8. Photosensitization of ROS by P-Pc-Cbz Surface. The ROS produced by sensitization can be generated via two photodynamic pathways known as type I and type II. In the type I mechanism, the triplet excited state of the PS (^{3}PS*) achieved after photon absorption transfers electrons to surrounding biological substrates leading to the formation of free radicals. In the presence of oxygen, these ones generate $O_2^{\cdot-}$, which can dismute into H_2O_2, the precursor of hydroxyl radicals ($OH^{\cdot}$). On the other hand, in the type II photomechanism, the ^{3}PS* transfers energy to molecular oxygen producing $^1O_2$.[58]

A crucial aspect to be considered in the design of antimicrobial coatings is their capability to photogenerate $^1O_2$. This ROS produced by a type II pathway[58] is a desired bactericidal agent that plays a key role in the inactivation of microorganisms. With high oxidative power and reactivity, this ROS can nonspecifically damage an extensive range of biomolecules, such as proteins, lipids, nucleic acids, etc.[59] Hence, the evaluation of the photodynamic properties of **P-Pc-Cbz** was first studied considering its ability to produce $^1O_2$

https://doi.org/10.1021/acsapm.2c01890
ACS Appl. Polym. Mater. 2023, 5, 943−956

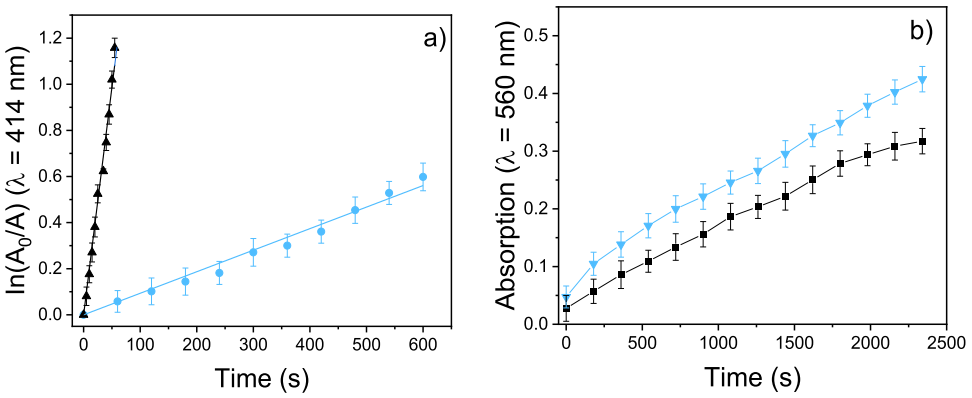

Figure 8. (a) Pseudo-first-order kinetic data fitting for the oxidation of DPBF with $^1O_2$ photosensitized by **P-Pc-Cbz** (black up-pointing triangle) and **Pc-Cbz** (blue circle) in DMF. (b) Photogeneration of $O_2^{\cdot-}$ detected by NBT reduction monitored by following the increase in the absorbance at λ = 560 nm in function of time. Samples contain **P-Pc-Cbz**, NBT, and NADH (blue down-pointing triangle); and NBT and NADH (black square). [NBT] = 0.2 mM and [NADH] = 0.5 mM. λirr = 455−800 nm.

under light irradiation. This assessment was carried out through an indirect method using DPBF as a chemical trap of $^1O_2$. The scavenger reacts with $^1O_2$ to produce the endoperoxide derivative, which decomposes spontaneously (see Figure S7). Thus, the formation of $^1O_2$ can be monitored by following the decrease of the absorption band of DPBF at 414 nm.[60]

The polymeric film **P-Pc-Cbz** was dipped in an air-equilibrated solution of DPBF in DMF, and it was then exposed to visible light irradiation (455−800 nm). In addition, the photooxidation reaction of the trapping reagent was also assessed and compared using a solution of **Pc-Cbz** in DMF. The spectroscopic changes corresponding to the consumption of DPBF photosensitized **P-Pc-Cbz** are shown in Figure S7. The absorption band of DPBF exhibited a gradual decrease for both systems, evidencing that they can generate $^1O_2$ after light irradiation. Both materials were photostable along the kinetic measurements.

The spectroscopy decay of DPBF induced by the photosensitizing action of **Pc-Cbz** and **P-Pc-Cbz** at different irradiation times follows a pseudo-first-order kinetic (Figure 8a). As can be appreciated in the semilogarithmic plot, DPBF photooxidation shows different rates for these materials as demonstrated by the values of the k_{obs}, which were obtained from the slope of the linear fit and are grafted in Table S2. The photogeneration of $^1O_2$ by **P-Pc-Cbz** is one order of magnitude slower than the monomer in solution. This value is reasonable because $^1O_2$ production photosensitized by **P-Pc-Cbz** occurs only on the surface of the light-activable material. It is worth mentioning that porphycene-based polymeric surfaces may be a more efficient antimicrobial material than those holding porphyrin as light absorber. This is because the higher molar extinction coefficients of porphycenes (typical extinction coefficient ~10^4 and ~10^3 for porphyrin) compensate for their lower $^1O_2$ production yields in relation to porphyrins. These outcomes not only demonstrated that **P-Pc-Cbz** undergoes a type II photoprocess under light irradiation but also it is a promising preliminary indication that the **P-Pc-Cbz** would act as an effective photoactivable bactericidal surface.

The capability of materials to photogenerate $^1O_2$ is considered a key factor for their application in antimicrobial systems; however, it is not the only ROS capable of producing damages in the cellular compartments. To evaluate the presence of other types of ROS generated by a type I mechanism,[58] the formation of $O_2^{\cdot-}$ was determined using the NBT method (see Figure S8). Here, NBT reacts with $O_2^{\cdot-}$ to produce diformazan, which can be spectroscopically monitored by following its absorption band at 560 nm. This reaction is favored by polar solvents and the presence of reducing agents like NADH.[61,62]

P-Pc-Cbz surface dipped in a solution containing NBT and NADH was irradiated with visible light (455−800 nm) under aerobic conditions. Absorption spectra acquired at different irradiation times showed a slight gradual increase of the absorption band of diformazan, indicating that $O_2^{\cdot-}$ is generated by the electrodeposited polymer. Figure S8 shows representative results using **P-Pc-Cbz** as photosensitizing material.

Figure 8b shows the reduction of NBT induced by **P-Pc-Cbz** as a function of the irradiation time. NADH-mediated $O_2^{\cdot-}$ formation did not take place in control experiments: the absence of NADH or **P-Pc-Cbz** in the dark. However, the reduction of NBT photomediated by **P-Pc-Cbz** shows an increase in the diformazan production compared to the NBT + NADH control. This outcome is in agreement with the capability of the **Pc-Cbz** monomer to photogenerate ROS through a type I photodynamic mechanism.[33]

By comparing the values obtained for the polymer and the control, it can be inferred that the generation capacity of $O_2^{\cdot-}$ by **P-Pc-Cbz** is not efficient, indicating that the polymeric surface presents a low capacity to accept electrons. It is known that PSs with the ability to accept electrons produce ROS species mainly by type I pathway; otherwise, the favored mechanism will be type II (generation of $^1O_2$).[63] In addition, tetrapyrrolic macrocycles demonstrate a type II mechanism predominantly.[64]

Nevertheless, despite the low result obtained from this photoinduced reaction, the irradiation of **P-Pc-Cbz** films also leads to the formation of $O_2^{\cdot-}$ (type I pathway). This ROS is the significant importance since it can be converted to the highly reactive hydroxyl radical in the cellular environment, which is known as Fenton chemistry.[65] Photodynamic studies demonstrate that the porphycene-based antimicrobial surface produces ROS by both type I and type II photoprocess after light irradiation although **P-Pc-Cbz** is mainly efficient sensitizer of $^1O_2$.

https://doi.org/10.1021/acsapm.2c01890
ACS Appl. Polym. Mater. 2023, 5, 943−956

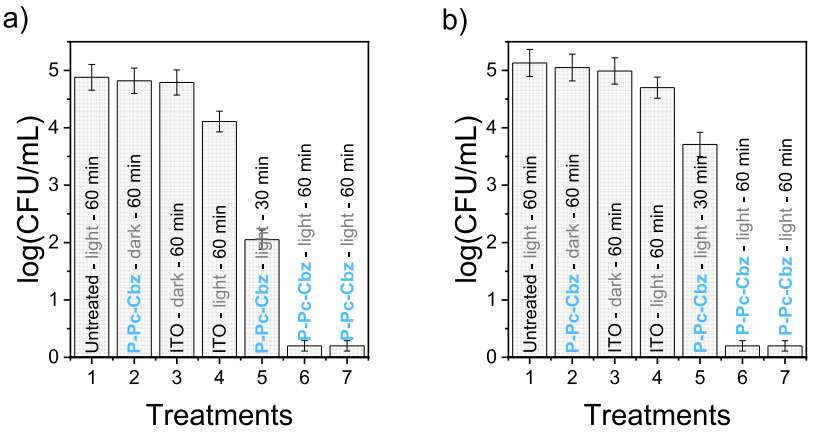

Figure 9. Survival curves of (a) MRSA and (b) *E. coli* cell suspensions (~10^5 CFU/mL) in PBS. Treatment: (1) initial control. Untreated cells irradiated for 60 min. (2) Cells deposited on **P-Pc-Cbz** and kept in the dark for 60 min. (3) Cells deposited on ITO and kept in the dark for 60 min. (4) Cells deposited on ITO and irradiated 60 min. (5) Cells deposited on **P-Pc-Cbz** and irradiated 30 min. (6) Cells deposited on **P-Pc-Cbz** and irradiated 60 min. (7) Second PDI cycle, cells deposited on **P-Pc-Cbz** and irradiated 60 min. Samples were irradiated with visible light (350–800 nm).

3.9. Photostability. The photostability of antimicrobial surfaces is a crucial parameter to be considered in order to determine the real practical applications of these materials. The coating must be sufficiently resistant to photobleaching to completely eradicate the pathogens and allow its reutilization. **P-Pc-Pcz** photodegradation was measured by acquiring UV–visible spectra of the polymeric films dipped in air-equilibrated PBS solution after visible light irradiation, monitoring the decrease of the Soret band intensity (λ = 393 nm). Irradiation conditions were the same used for PDI assessments. Figure S9 shows the spectroscopic changes of **P-Pc-Pcz** induced by the photooxidation processes as a function of the irradiation time. After 3 h, a photodegradation of 22% was observed for **P-Pc-Cbz**, evidencing substantial photostability for reusability and practical uses, which is crucial in view of the antimicrobial applications envisaged.

The photodecomposition of the self-sterilizing surface in PBS was observed to follow a first-order kinetic model (Figure S10). The observed rate constant of photobleaching (k_{obs}^{P}) obtained from the slope ($k_{obs}^{P} = (139 \pm 2) \times 10^{-5}$ min^{-1}) was employed to calculate the photobleaching half-life time ($\tau_{1/2}$) using eq S1. Under these experimental conditions, a $\tau_{1/2}$ value of 500 min was determined for **P-Pc-Pcz**. Even though $\tau_{1/2}$ values cannot be directly compared due to the different experimental conditions, we hoped that these films were more photostable than the electrogenerated films based on previously reported porphyrins since porphycenes are more difficult to oxidize than their porphyrin counterparts.[22,24] However, porphycene-based film showed similar photostability that electrodeposited porphyrins measured under similar conditions.[12] It is noteworthy that the photoactive porphycene units are immersed in the polymeric matrix, which could give them some protective effect against the damaging effect of the ROS.

P-Pc-Cbz polymer was not dissolved or released to the medium throughout the entire kinetic experiment, which was proved by the absence of its characteristic absorption bands in the acquired spectra. Furthermore, as a most sensitive technique, fluorescence measurements confirmed that PS desorption to the environment does not occur. Thus, these experiments disclose the irreversible adsorption of the polymer on the surface without PS desorption processes.

3.10. Antimicrobial Action of P-Pc-Cbz. Encouraged by the results obtained from the photodynamic and photobleaching studies, we decided to evaluate the ability of this porphycene-based material to act as an antimicrobial surface. The photoinactivation ability of this light-activated polymeric film was assessed in vitro against MRSA and *E. coli* bacterial suspensions. These strains were chosen since they are responsible for nosocomial infections. They are considered a severe threat to human health care and have acquired resistance to the available antibiotics. Moreover, these microorganisms can form biofilms on a wide range of medical instruments and hospital-associated facilities, increasing the risk of transmitting resistant strains.

PDI treatments were investigated by dipping two square surfaces of **P-Pc-Cbz** (0.09 cm^2) into 200 μL of bacterial suspension (~10^5 CFU/mL), which were irradiated with visible light for 30 and 60 min. Therapy results are shown in Figure 9. First, Figure 9a shows the survival of MRSA after different irradiation times. Control assessments showed that the viability of MRSA was not affected by keeping the bacterial suspension in the dark for 60 min in the presence of ITO and **P-Pc-Cbz** (Figure 9a, Treatments 2 and 3). A slight inactivation (<1 log) was observed for MRSA cells after 60 min of irradiation on the ITO electrode (Figure 9a, Treatment 4). Similar reductions in cell viability were found in the literature.[11,12] In addition, no toxicity was found for untreated cells and irradiated for 60 min (Figure 9a, Treatment 1). On the other hand, pathogenic microorganisms were inactivated by the polymeric material after visible light irradiation. All these results prove that MRSA mortality is due to the photosensitizing effect of **P-Pc-Cbz**. The efficiency of the photokilling was dependent on the irradiation time. The photodynamic action of the polymeric surface generates almost 3 log decrease in bacterial survival after 30 min of exposure to visible light. This outcome signifies a photoinactivation of MRSA higher than 99.85% (Figure 9a, Treatment 5). Moreover, no colony formation was observed after 60 min of irradiation (Figure 9a, Treatment 6). This reduction represents a value higher than 99,998% cell viability, demonstrating that **P-Pc-Cbz** is a promising photoactivable antimicrobial surface to treat this strain.

https://doi.org/10.1021/acsapm.2c01890
ACS Appl. Polym. Mater. 2023, 5, 943–956

Table 1. Electrodeposited Polymers Applied in Antimicrobial Photodynamic Therapy

electropolymers	bacterial strain	bacterial density (CFU/mL)	fluent energy (J/cm^2)[a]	inactivation %	ref
PEDOT-C_{60}	*S. aureus*	~10^4	324	>99.9	11
TFA-Po	*E. coli*	~10^6	162	>99.9	68
	C. albicans		162	>99.7	
Cbz-Po-C_{60}	*S. aureus*	~10^4	162	>99.96	19
	E. coli		324	>99.98	
Cbz-Den-Po	*S. aureus*	~10^4	162	>99.9998	12
	E. coli		162	>99.4%	
PEDOT-Zn-Porph + KI	*S. aureus*	~10^4	108	>99.98	70
	E. coli		162	>99.98	
PEDOT-Cu-Porph + KI	*S. aureus*	~10^4	108	>99.98	70
	E. coli		162	>95	
Zn-Porph-NH_2	*S. aureus*			>99.8	69
P-Pc-Cbz	MRSA	~10^5	324	>99.998	this work
	E. coli		324	>99.998	

[a]Visible light.

Motivated by these findings, we decided to extend the work by studying the photoinactivation of the Gram-negative *E. coli* bacteria. As shown in Figure 9b, control experiments showed similar behavior to MRSA in the dark treatments (Figure 9b, Treatments 2 and 3). In addition, the survival of *E. coli* was unaffected by irradiation for 60 min (Figure 9b, Treatment 1), and a slight photokilling (<0.5 log) was produced after 60 min of irradiation in the presence of an ITO electrode (Figure 9b, Treatment 4). However, a remarkable decrease in the viability of *E. coli* cells was observed in the presence of the polymeric surfaces. After 30 min of irradiation with visible light, the photodynamic activity of **P-Pc-Cbz** produces a ~1.4 log decrease in *E. coli* survival, representing a photoinactivation higher than 96% (Figure 9b, Treatment 5). This result indicates a lower antimicrobial action than that achieved over MRSA, and it can be explained considering that Gram-negative bacteria are more challenging to kill than Gram-positive due to the nature of the bacterial cell envelope.[66] The outer cell wall of Gram-negative bacteria constituted by a complex multilayer structure with porin-acting proteins works as a permeability barrier that impedes ROS penetration. Nevertheless, complete bacterial inactivation (>99.998%) was achieved after 60 min of irradiation (Figure 9b, Treatment 6).

The complete elimination of both bacteria strains (MRSA and *E. coli*) was achieved by the photosensitization of **P-Pc-Cbz** after 60 min. Thus, our polymeric material can be considered antimicrobial since the American Society of Microbiology proposed that this term be used when the new material reaches a decrease of at least 3 log in CFU, i.e. cell death higher than 99.9%.[67] PDI outcomes demonstrate that **P-Pc-Cbz** polymeric films are efficient self-sterilizing and antimicrobial surfaces with potential application in the design of medical devices, coating of healthcare surfaces, and water decontamination, among other ROS-mediated applications. Up to date, there is no evidence of porphycene-based polymers activated by visible light in the PDI of microorganisms. Thus, we are starting to pave the way for the preparation of promising antimicrobial materials.

The comparison of the antimicrobial activity of **P-Pc-Cbz** with other electrodeposited surfaces is problematic mainly due to the different experimental conditions, such as bacterial strains, bacterial density, wavelength irradiation, treatment procedure, nature and concentration of the PS, light dosage, etc. Table 1 compares the PDI treatments of previously published works using electrodeposited polymeric surfaces. A detailed analysis of Table 1 reveals that the PDI of bacteria sensitized by an electrodeposited PEDOT-fullerene C_{60} (PEDOT-C_{60}) polymeric film was less effective to inactive *S. aureus*.[11] **P-Pc-Cbz** produced a higher inactivation at similar times. Furthermore, **P-Pc-Cbz** presented better antimicrobial performance than previous reports of electropolymers obtained from triphenylamine-porphyrin (TFA-Po) and carbazol-porphyrin-fullerene C_{60} (Cbz-Po-C_{60}) monomers.[12,19,68] Also, **P-Pc-Cbz** showed a better performance than our previously reported carbazole-dendrimeric porphyrin (Cbz-Den-Po) to photokill *E. coli*. The higher absorption of porphycene in the visible region compared to porphyrins and fullerenes could be responsible for this outstanding bactericidal action.

On the other hand, metal phthalocyanine complexes, which are tetrapyrrolic macrocycles with high red absorption, were also electrodeposited on ITO electrodes and evaluated in vitro.[69,70] Blacha-Grzechnik and co-workers prepared a photoactive biocidal layer by an electrochemical oxidative process of a zinc (tetraamino)phthalocyanine (Zn-Porph-NH_2), which produced an inhibition of 99.8% *S. aureus* after visible light irradiation.[69] Finally, Durantini and co-workers evaluated two electrodeposited polymers using two metal phthalocyanine complexes (PEDOT-Zn-Porph and PEDOT-Cu-Porph); contrary to what was expected, they exhibited lower antimicrobial capacity. Even more, the PDI treatments had to be potentiated with an inorganic salt (KI) to improve their efficiency and reach similar antimicrobial properties to our system.[70] Thus, **P-Pc-Cbz** light-activated coating not only has promising biocidal action but also a higher performance on both strains than the above-mentioned electropolymers.

Inspired by these findings and having in mind to study the stability and reusability of **P-Pc-Cbz**, the reuse of surfaces was assessed for both antibiotic-resistant strains in new PDI treatments. After removing and washing the polymeric films, these were dipped in a fresh bacterial suspension and irradiated with visible light for 60 min. Cell survivals corresponding to the second PDI cycle are shown in Figure 9a (Treatment 7) and Figure 9b (Treatment 7) for MRSA and *E. coli*, respectively. As can be observed, the photoinactivation in both strains was similar to the first treatment without a significant difference in cell survival (photokilling activity >99.998). Thus, **P-Pc-Cbz** can be removed, recovered, and reused in a new treatment, conserving its photoactivity and

https://doi.org/10.1021/acsapm.2c01890
ACS Appl. Polym. Mater. 2023, 5, 943−956

antimicrobial action. After each PDI assay, absorption and fluorescence spectra disclosed that the bacterial suspensions were not contaminated with porphycene.

Based on the in vitro studies, it can be stated that the designed polymeric surface could act as a promising material to maintain asepsis in clinical settings. Thus, the alternatives to the orthodox and practically exclusive methodology of applying disinfectants to sterilize surfaces are diversified. This is vital in the current microbiological crisis since there is a relationship between the sterilization of surfaces using disinfectants and the appearance of resistant bacteria.

4. CONCLUSIONS

An appropriate and straightforward approach to fabricate light-activated antimicrobial surfaces was developed. This method was based on the electrochemical polymerization of a dual-functional monomer. The controllable and facile electrodeposition process through carbazole moieties led to the formation of films with porphycene nuclei fixed in the **P-Pc-Cbz** polymer structure. The material was obtained as homogenous thin films over Pt and ITO surfaces. Spectroscopic, electrochemical, and spectroelectrochemical studies demonstrated that the porphycene structure is not modified throughout the electropolymerization procedure, retaining its photophysical and photodynamic features. Thus, the photoactivable films can produce ROS by type I and type II photoreactions after visible light irradiation. On the other hand, the photodynamic polymer was highly resistant to photobleaching, thanks to the high photostability of this kind of tetrapyrrolic macrocycle.

The antimicrobial action of the porphycene-based polymer was assessed in vitro against Gram-positive and Gram-negative bacteria models. PDI treatments showed a complete photokilling of *S. aureus* and *E. coli* bacterial suspensions after 60 min of visible light irradiation. Therefore, **P-Pc-Cbz** polymeric surfaces can be considered as antimicrobial/antibacterial photoactivable coating. Consequently, our investigations provide the first report of a porphycene-based polymeric material with highly efficient antimicrobial activity.

We hope this photoactive self-sterilizing coating produces a great impulse in the development of antimicrobial films using porphycenes. Finally, **P-Pc-Cbz** is a potential polymer that can be used to control microbial proliferation, conserving aseptic conditions. In addition, it could be applied in other ROS-mediated applications like disinfection of contaminated water suspension. **P-Pc-Cbz** could be dipped in microbiologically-contaminated water, irradiated, and then easily recovered/removed and reused. Finally, considering that **P-Pc-Cbz** presents a high absorption in the red region of the electromagnetic spectrum, it could be more efficient to capture light in turbid/contaminated suspensions.

■ ASSOCIATED CONTENT

Supporting Information

The Supporting Information is available free of charge at https://pubs.acs.org/doi/10.1021/acsapm.2c01890.

A total of 10 figures, one scheme, one equation, and two tables are listed in the supporting files (PDF)

■ AUTHOR INFORMATION

Corresponding Authors

Javier E. Durantini − *IITEMA-CONICET, Departamento de Química, Facultad de Ciencias Exactas Físico-Químicas y Naturales, Universidad Nacional de Río Cuarto, X5804BYA Río Cuarto, Córdoba, Argentina*; Phone: +54 358 4676538; Email: jdurantini@exa.unrc.edu.ar; Fax: +54 358 76233

Daniel A. Heredia − *IDAS-CONICET, Departamento de Química, Facultad de Ciencias Exactas Físico-Químicas y Naturales, Universidad Nacional de Río Cuarto, X5804BYA Río Cuarto, Córdoba, Argentina*; orcid.org/0000-0002-0667-3906; Phone: +54 358 4676538; Email: dheredia@exa.unrc.edu.ar; Fax: +54 358 76233

Authors

Edwin J. Gonzalez Lopez − *IDAS-CONICET, Departamento de Química, Facultad de Ciencias Exactas Físico-Químicas y Naturales, Universidad Nacional de Río Cuarto, X5804BYA Río Cuarto, Córdoba, Argentina*

Melisa Renfige Rodriguez − *IITEMA-CONICET, Departamento de Química, Facultad de Ciencias Exactas Físico-Químicas y Naturales, Universidad Nacional de Río Cuarto, X5804BYA Río Cuarto, Córdoba, Argentina*

Sofia C. Santamarina − *IDAS-CONICET, Departamento de Química, Facultad de Ciencias Exactas Físico-Químicas y Naturales, Universidad Nacional de Río Cuarto, X5804BYA Río Cuarto, Córdoba, Argentina*

Lorena Macor − *IITEMA-CONICET, Departamento de Química, Facultad de Ciencias Exactas Físico-Químicas y Naturales, Universidad Nacional de Río Cuarto, X5804BYA Río Cuarto, Córdoba, Argentina*

Luis A. Otero − *IITEMA-CONICET, Departamento de Química, Facultad de Ciencias Exactas Físico-Químicas y Naturales, Universidad Nacional de Río Cuarto, X5804BYA Río Cuarto, Córdoba, Argentina*

Miguel A. Gervaldo − *IITEMA-CONICET, Departamento de Química, Facultad de Ciencias Exactas Físico-Químicas y Naturales, Universidad Nacional de Río Cuarto, X5804BYA Río Cuarto, Córdoba, Argentina*; orcid.org/0000-0001-9287-5872

Andrés M. Durantini − *IDAS-CONICET, Departamento de Química, Facultad de Ciencias Exactas Físico-Químicas y Naturales, Universidad Nacional de Río Cuarto, X5804BYA Río Cuarto, Córdoba, Argentina*; orcid.org/0000-0002-7898-4033

Edgardo N. Durantini − *IDAS-CONICET, Departamento de Química, Facultad de Ciencias Exactas Físico-Químicas y Naturales, Universidad Nacional de Río Cuarto, X5804BYA Río Cuarto, Córdoba, Argentina*; orcid.org/0000-0001-8901-7543

Complete contact information is available at: https://pubs.acs.org/10.1021/acsapm.2c01890

Author Contributions

The manuscript was written through contributions of all authors. All authors have given approval to the final version of the manuscript.

Funding

This research was funded by ANPCYT (PICT-2016-2370, PICT-2016-0667), CONICET (PIP-2015 1122015 0100197 CO), and SECYT-UNRC (PPI-2020 Res. 083/20).

Notes

The authors declare no competing financial interest.

■ ACKNOWLEDGMENTS

Authors are grateful to Consejo Nacional de Investigaciones Científicas y Técnicas (CONICET, PIP-2015 1122015 0100197 CO) of Argentina, SECYT Universidad Nacional de Río Cuarto (PPI-2020 Res. 083/20), and Agencia Nacional de Promoción Científica y Tecnológica (FONCYT, PICT-2016-2370, PICT-2016-0667) for financial support. L.P.M., L.A.O., M.A.G., E.N.D., A.M.D., J.E.D., and D.A.H. are scientific members of CONICET. E.J.G.L., S.C.S., and M.Y.R.R. thank CONICET for doctoral fellowship.

■ REFERENCES

(1) Iskandar, K.; Murugaiyan, J.; Hammoudi Halat, D.; Hage, S. E.; Chibabhai, V.; Adukkadukkam, S.; Roques, C.; Molinier, L.; Salameh, P.; Van Dongen, M. Antibiotic Discovery and Resistance: The Chase and the Race. *Antibiotics* **2022**, *11*, 182.

(2) Radhouani, H.; Silva, N.; Poeta, P.; Torres, C.; Correia, S.; Igrejas, G. Potential Impact of Antimicrobial Resistance in Wildlife, Environment, and Human Health. *Front. Microbiol.* **2014**, *5*, 23.

(3) *New report calls for urgent action to avert antimicrobial resistance crisis*; World Health Organization. https://www.who.int/news/item/29-04-2019-new-report-calls-for-urgent-action-to-avert-antimicrobial-resistance-crisis (accessed March 2022).

(4) Ran, B.; Wang, Z.; Cai, W.; Ran, L.; Xia, W.; Liu, W.; Peng, X. Organic Photo-Antimicrobials: Principles, Molecule Design, and Applications. *J. Am. Chem. Soc.* **2021**, *143*, 17891−17909.

(5) Maan, A. M. C.; Hofman, A. H.; Vos, W. M.; Kamperman, M. Recent Developments and Practical Feasibility of Polymer-Based Antifouling Coatings. *Adv. Funct. Mater.* **2020**, *30*, No. 2000936.

(6) Comuzzi, C.; Marino, M.; Poletti, D.; Boaro, M.; Strazzolini, P.; New Antimicrobial, P. V. C. Composites Porphyrins Self-Aggregation in Tuning Surface Morphologies and Photodynamic Inactivation Towards Sustainable Water Disinfection. *J. Photochem. Photobiol. A* **2022**, *430*, No. 113967.

(7) Spagnul, C.; Turner, L. C.; Boyle, R. W. Immobilized Photosensitizers for Antimicrobial Applications. *J. Photochem. Photobiol. B: Biol.* **2015**, *150*, 11−30.

(8) Mesquita, M. Q.; Dias, C. Q.; Neves, M. G. P. M. S.; Almeida, A.; Faustino, M. A. S. Revisiting Current Photoactive Materials for Antimicrobial Photodynamic Therapy. *Molecules* **2018**, *23*, 2424.

(9) Youf, R.; Müller, M.; Balasini, A.; Müller, F. T. M.; Hascoët, A.; Jonas, U.; Schönherr, H.; Lemercier, G.; Montier, T.; Gall, T. L. Antimicrobial Photodynamic Therapy: Latest Developments with a Focus on Combinatory Strategies. *Pharmaceutics* **2021**, *13*, 1995.

(10) Hamblin, M. R. Antimicrobial Photodynamic Inactivation: A Bright New Technique to Kill Resistant Microbes. *Curr. Opin. Microbiol.* **2016**, *33*, 67−73.

(11) Reynoso, E.; Durantini, A. M.; Solis, C. A.; Macor, L. P.; Otero, L. A.; Gervaldo, M. A.; Durantini, E. N.; Heredia, D. A. Photoactive Antimicrobial Coating Based on a Pedot-Fullerene C_{60} Polymeric Dyad. *RSC Adv.* **2021**, *11*, 23519−23532.

(12) Heredia, D. A.; Martinez, S. R.; Durantini, A. M.; Pérez, M. E.; Mangione, M. I.; Durantini, J. E.; Gervaldo, M. A.; Otero, L. A.; Durantini, E. N. Antimicrobial Photodynamic Polymeric Films Bearing Biscarbazol Triphenylamine End-Capped Dendrimeric Zn(II) Porphyrin. *ACS Appl. Mater. Interfaces* **2019**, *11*, 27574−27587.

(13) Blacha-Grzechnik, A.; Krzywiecki, M.; Motyka, R.; Czichy, M. Electrochemically Polymerized Terthiopehene−C_{60} Dyads for the Photochemical Generation of Singlet Oxygen. *J. Phys. Chem. C* **2019**, *123*, 25915−25924.

(14) Nyga, A.; Motyka, R.; Bussetti, G.; Calloni, A.; Jagadeesh, M. S.; Fijak, S.; Pluczyk-Malek, S.; Data, P.; Blacha-Grzechnik, A. Electrochemically Deposited Poly(Selenophene)-Fullerene Photoactive Layer: Tuning of the Spectroscopic Properties Towards Visible Light-Driven Generation of Singlet Oxygen. *Appl. Surf. Sci.* **2020**, *525*, No. 146594.

(15) Blacha-Grzechnik, A.; Piwowar, K.; Zdyb, T.; Krzywiecki, M. Formation Of Poly(Azure A)-C_{60} Photoactive Layer as a Novel Approach in The Heterogeneous Photogeneration of Singlet Oxygen. *Appl. Surf. Sci.* **2018**, *457*, 221−228.

(16) Heredia, D.; Fernandez, L.; Otero, L.; Ichikawa, M.; Lin, C.-Y.; Liao, Y.-L.; Wang, S.-A.; Wong, K.-T.; Fungo, F. Electrochemical Tuning of Morphological and Optoelectronic Characteristics of Donor−Acceptor Spiro-Fluorene Polymer Film. Application in the Building of an Electroluminescent Device. *J. Phys. Chem. C* **2011**, *115*, 21907−21914.

(17) Heredia, D. A.; Gonzalez Lopez, J. E.; Durantini, E. N.; Durantini, J. E.; Dittrich, T.; Rappich, J.; Macor, L.; Solis, C.; Morales, G. M.; Gervaldo, M.; Otero, L. Electrochemical, Spectroelectrochemical and Surface Photovoltage Study of Ambipolar C_{60}-EDOT and C_{60}-Carbazole Based Conducting Polymers. *Electrochim. Acta* **2019**, *311*, 178−191.

(18) Comuzzi, C.; Fiorot, A.; Baggio, A.; Maifreni, M.; Strazzolini, P.; Marino, M.; Susmel, S. Imprinting Pentaphyrin on Conductive Electropolymerized Dipyrromethane Films: A New Strategy towards the Synthesis of Photokilling Materials. *ChemPlusChem* **2020**, *85*, 776−782.

(19) Ballatore, M. B.; Durantini, J. E.; Gsponer, N. S.; Suarez, M. B.; Gervaldo, M.; Otero, L.; Spesia, M. B.; Milanesio, M. E.; Durantini, E. N. Photodynamic Inactivation of Bacteria Using Novel Electrogenerated Porphyrin-Fullerene C_{60} Polymeric Films. *Environ. Sci. Technol.* **2015**, *49*, 7456−7463.

(20) Anguera, G.; Sánchez-García, D. Porphycenes and Related Isomers: Synthetic Aspects. *Chem. Rev.* **2017**, *117*, 2481−2516.

(21) Vogel, E.; Köcher, M.; Schmickler, H.; Lex, J. Porphycene-a Novel Porphin Isomer. *Angew. Chem., Int. Ed.* **1986**, *25*, 257−259.

(22) Waluk, J. Spectroscopy and Tautomerization Studies of Porphycenes. *Chem. Rev.* **2017**, *117*, 2447−2480.

(23) Rao, S. V.; Prashant, T. S.; Swine, D.; Sarma, T.; Panda, P. K.; Tewari, S. P. Two-Photon and Three-Photon Absorption in Dinaphthoporphycenes. *Chem. Phys. Lett.* **2011**, *514*, 98−103.

(24) Rubio, N.; Prat, F.; Bou, N.; Borrell, J. I.; Teixidó, J.; Villanueva, Á.; Juarranz, Á.; Cañete, M.; Stockert, J. C.; Nonell, S. A Comparison Between the Photophysical and Photosensitising Properties of Tetraphenyl Porphycenes and Porphyrins. *New J. Chem.* **2005**, *29*, 378−384.

(25) Arnbjerg, J.; Jiménez-Banzo, A.; Paterson, M. J.; Nonell, S.; Borrell, J. I.; Christiansen, O.; Ogilby, P. R. Two-Photon Absorption in Tetraphenylporphycenes: Are Porphycenes Better Candidates than Porphyrins for Providing Optimal Optical Properties for Two-Photon Photodynamic Therapy? *J. Am. Chem. Soc.* **2007**, *129*, 5188−5199.

(26) Pati, N. N.; Kumar, B. S.; Sivadasan, D.; Sahoo, S. S.; Panda, P. K. Unsymmetrical Bipyrrole Derived Highly Soluble and Emissive β-Dialkylporphycenes with Good Singlet Oxygen Generation Ability. *J. Porphyrins Phthalocyanines* **2020**, *24*, 121−128.

(27) Rana, A.; Panda, P. K. β-Octamethoxyporphycenes. *Org. Lett.* **2014**, *16*, 78−81.

(28) Stockert, J. C.; Cañete, M.; Juarranz, A.; Villanueva, A.; Horobin, R. W.; Borrell, J. I.; Teixidó, J.; Nonell, S. Porphycenes: Facts and Prospects in Photodynamic Therapy of Cancer. *Curr. Med. Chem.* **2007**, *14*, 997−1026.

(29) Wang, Y.; Pan, Z.; Cheng, X. L.; Zhang, K.; Zhang, X.; Qin, Y.; Fan, J.; Yan, T.; Han, T.; Shiu, K. K.; Chun-KitHau, S.; Mak, N.-K.; Daniel, W. J. K.; Liu, X.; Li, M.; Deng, G.; Zheng, Q.; Lu, J.; Li, D. A Red-Light-Activated Sulfonamide Porphycene for Highly Efficient Photodynamic Therapy against Hypoxic Tumor. *Eur. J. Med. Chem.* **2021**, *209*, No. 112867.

(30) Masiera, N.; Bojarska, A.; Gawryszewska, I.; Sadowy, E.; Hryniewicz, W.; Waluk, J. Antimicrobial Photodynamic Therapy by Means of Porphycene Photosensitizers. *J. Photochem. Photobiol. B: Biol.* **2017**, *174*, 84−89.

(31) Ruiz-González, R.; Agut, M.; Reddi, E.; Nonell, S. A Comparative Study on Two Cationic Porphycenes: Photophysical

https://doi.org/10.1021/acsapm.2c01890
ACS Appl. Polym. Mater. 2023, 5, 943−956

and Antimicrobial Photoinactivation Evaluation. *Int. J. Mol. Sci.* **2015**, *16*, 27072−27086.
(32) Masiera, N.; Ostapko, J.; Gorski, A.; Bojarska, A.; Gawryszewska, I.; Sadowy, E.; Hryniewicz, W.; Waluk, J. Photoeradication of Bacteria with Porphycenes: Substituent Effects on The Efficiency. *Eur. J. Med. Chem.* **2020**, *200*, No. 112472.
(33) Gonzalez Lopez, E. J.; Santamarina, S. C.; Alvarez, M. G.; Heredia, D. A.; Durantini, E. N. Porphycenes as Broad-Spectrum Antimicrobial Photosensitizers. Potentiation with Potassium Iodide. *J. Photochem. Photobiol., A* **2023**, *435*, No. 114288.
(34) Ono, T.; Shinjo, H.; Koga, D.; Hisaeda, Y. Synthesis of a meso-Tetraalkylporphycene Bearing Reactive Sites: Toward Porphycene-Polydimethylsiloxane Hybrids with Enhanced Photophysical Properties. *Eur. J. Org. Chem.* **2019**, *46*, 7578−7583.
(35) Abe, M.; Futagawa, H.; Ono, T.; Yamada, T.; Kimizuka, N.; Hisaeda, Y. An Electropolymerized Crystalline Film Incorporating Axially-Bound Metalloporphycenes: Remarkable Reversibility, Reproducibility, and Coloration Efficiency of Ruthenium(II/III)-Based Electrochromism. *Inorg. Chem.* **2015**, *54*, 11061−11063.
(36) Sarma, T.; Panda, P. K. Annulated Isomeric, Expanded, and Contracted Porphyrins. *Chem. Rev.* **2017**, *117*, 2785−2838.
(37) Ganapathi, E.; Chatterjee, T.; Ravikanth, M. Facile Synthesis of 9,10,19,20-Tetraarylporphycenes. *Eur. J. Org. Chem.* **2014**, *30*, 6701−6706.
(38) Ono, T.; Xu, N.; Koga, D.; Ideo, T.; Sugimoto, M.; Hisaeda, Y. Gram-Scale Synthesis of Porphycenes through Acid-Catalyzed Oxidative Macrocyclizations of E/Z Mixed 5,6-Diaryldipyrroethenes. *RSC Adv.* **2018**, *8*, 39269−39273.
(39) Solis, C.; Durantini, J. E.; Macor, L.; Heredia, D. A.; Gonzalez Lopez, J. E.; Durantini, E. N.; Mangione, M. I.; Rappich, J.; Dittrich, T.; Otero, L.; Gervaldo, M. Electrochemical Formation of Photoactive Organic Heterojunctions. Porphyrin-C_{60} Polymeric Photoelectrochemical Cells. *Electrochim. Acta* **2021**, *365*, No. 137333.
(40) Zhang, H.; Zhang, Y.; Gu, C.; Ma, Y. Electropolymerized Conjugated Microporous Poly (Zinc-Porphyrin) Films as Potential Electrode Materials in Supercapacitors. *Adv. Energy Mater.* **2015**, *5*, No. 1402175.
(41) Scanone, A. C.; Gsponer, N. S.; Alvarez, M. G.; Durantini, E. N. Porphyrins Containing Basic Aliphatic Amino Groups as Potential Broad-Spectrum Antimicrobial Agents. *Photodiagn. Photodyn. Ther.* **2018**, *24*, 220−227.
(42) Reynoso, E.; Quiroga, E. D.; Agazzi, M. L.; Ballatore, M. B.; Bertolotti, S. G.; Durantini, E. N. Photodynamic Inactivation of Microorganisms Sensitized by Cationic BODIPY Derivatives Potentiated by Potassium Iodide. *Photochem. Photobiol. Sci.* **2017**, *16*, 1524−1536.
(43) Kuzuhara, D.; Nakaoka, H.; Matsuo, K.; Aratani, N.; Yamada, H. 2,7,12,17-Tetra(2,5-Thienylene)-Substituted Porphycenes. *J. Porphyrins Phthalocyanines* **2019**, *23*, 898−907.
(44) Xu, N.; Ono, T.; Hisaeda, Y. Symmetry Reduction of Porphycenes with Finely Tuned Optical and Electronic Properties through Oxidative Cyclization of *E/Z*-Mixed Dipyrroethenes. *Chem. − Eur. J.* **2019**, *25*, 11680.
(45) Durantini, J. E.; Rubio, R.; Solis, C.; Macor, L.; Morales, G.; Mangione, M. I.; Heredia, D. A.; Durantini, E. N.; Otero, L.; Gervaldo, M. Electrosynthesis of a Hyperbranched Dendrimeric Porphyrin Polymer: Optical and Electronic Characterization as a Material for Bifunctional Electrochromic Supercapacitors. *Sustainable Energy Fuels* **2020**, *4*, 6125−6140.
(46) Li, M. C3-C3' and C6-C6' Oxidative Couplings of Carbazoles. *Chem. − Eur. J.* **2019**, *25*, 1142−1151.
(47) Hsiao, S.-H.; Lin, J.-W. Facile Fabrication of Electrochromic Poly(amine-amide) and Poly(amine-imide) Films Via Carbazole-Based Oxidative Coupling Electropolymerization. *Macromol. Chem. Phys.* **2014**, *215*, 1525−1532.
(48) Bard, A. J.; Faulkner, L. R. *Electrochemical Methods: Fundamentals and Applications*; 2nd Edition; Wiley & Sons: New York, 2001.
(49) Mangione, M. I.; Spanevello, R. A.; Minudri, D.; Heredia, D.; Fernandez, L.; Otero, L.; Fungo, F. Electropolimerization of Functionalizaed Carbazole End-Capped Dendrimers. Formation of Conductive Films. *Electrochim. Acta* **2016**, *207*, 143−151.
(50) Chen, J.; Shan, J.; Xu, Y.; Su, P.; Tong, L.; Yuwen, L.; Weng, L.; Bao, B.; Wang, L. Polyhedral Oligomeric Silsesquioxane (POSS)-Based Cationic Conjugated Oligoelectrolyte/Porphyrin for Efficient Energy Transfer and Multiamplified Antimicrobial Activity. *ACS Appl. Mater. Interfaces* **2018**, *10*, 34455−34463.
(51) Xing, C.; Xu, Q.; Tang, H.; Liu, L.; Wang, S. Conjugated Polymer/Porphyrin Complexes for Efficient Energy Transfer and Improving Light-Activated Antibacterial Activity. *J. Am. Chem. Soc.* **2009**, *131*, 13117−13124.
(52) Liu, L.; Chen, J.; Wang, S. Flexible Antibacterial Film Deposited with Polythiophene-Porphyrin Composite. *Adv. Healthcare Mater.* **2013**, *2*, 1582−1585.
(53) Rubio, N.; Borrell, J. I.; Teixido, J.; Canete, M.; Juarranz, A.; Villanueva, A.; Stockert, J. C.; Nonell, S. Photochemical Production and Characterisation of the Radical Ions of Tetraphenylporphycenes. *Photochem. Photobiol. Sci.* **2006**, *5*, 376−380.
(54) Kadish, K. M.; Boulas, P. L.; Kisters, M.; Vogel, E.; Aukauloo, A. M.; Souza, F. D.; Guilard, R. Synthesis and Electrochemical Reactivity of R-Bonded and *N*-Substituted Cobalt Porphycenes. *Inorg. Chem.* **1998**, *37*, 2693−2700.
(55) Gulam, R. M.; Matsushita, T.; Teraoka, J. Electronic and Vibrational Properties of Porphycene Anions. *J. Phys. Chem. A* **2003**, *107*, 2172−2178.
(56) Mangione, M. I.; Spanevello, R. A.; Rumbero, A.; Heredia, D.; Marzari, G.; Fernandez, L.; Otero, L.; Fungo, F. Electrogenerated Conductive Polymers from Triphenylamine End-Capped Dendrimers. *Macromolecules* **2013**, *46*, 4754−4763.
(57) Durantini, J.; Morales, G. M.; Santo, M.; Funes, M.; Durantini, E. N.; Fungo, F.; Dittrich, T.; Otero, L.; Gervaldo, M. Synthesis and Characterization of Porphyrin Electrochromic and Photovoltaic Electropolymers. *Org. Electron.* **2012**, *13*, 604−614.
(58) Baptista, M. S.; Cadet, J.; Di Mascio, P.; Ghogare, A. A.; Greer, A.; Hamblin, M. R.; Lorente, C.; Nunez, S. C.; Ribeiro, M. S.; Thomas, A. H.; Vignoni, M.; Yoshimura, T. M. Type I and Type II Photosensitized Oxidation Reactions: Guidelines and Mechanistic Pathways. *Photochem. Photobiol.* **2017**, *93*, 912−919.
(59) Cieplik, F.; Deng, D.; Crielaard, W.; Buchalla, W.; Hellwig, E.; Al-Ahmad, A.; Maisch, T. Antimicrobial photodynamic therapy − what we know and what we don't. *Crit. Rev. Microbiol.* **2018**, *44*, 571−589.
(60) Gonzalez Lopez, E. J.; Sarotti, A. M.; Martínez, S. M.; Macor, L. P.; Durantini, J. E.; Renfige, M.; Gervaldo, M. A.; Otero, L. A.; Durantini, A. M.; Durantini, E. N.; Heredia, D. A. BOPHY-Fullerene C_{60} Dyad as a Photosensitizer for Antimicrobial Photodynamic Therapy. *Chem. − Eur. J.* **2022**, *28*, No. e202103884.
(61) Maghzal, G. J.; Krause, K. H.; Stocker, R.; Jaquet, V. Detection of Reactive Oxygen Species Derived from the Family of NOX NADPH Oxidases. *Free Radical Biol. Med.* **2012**, *53*, 1903−1918.
(62) Rajendran, M. Quinones as Photosensitizer for Photodynamic Therapy: ROS Generation, Mechanism and Detection Methods. *Photodiagn. Photodyn. Ther.* **2016**, *13*, 175−187.
(63) Garcia-Diaz, M.; Huang, Y.-Y.; Hamblin, M. R. Use of Fluorescent Probes for ROS to Tease Apart Type I and Type II Photochemical Pathways in Photodynamic Therapy. *Methods* **2016**, *109*, 158−166.
(64) Sharma, S. K.; Chiang, L. Y.; Hamblin, M. R. Photodynamic therapy with fullerenes in vivo: reality or a dream? *Nanomedicine* **2011**, *6*, 1813−1825.
(65) Krumova, K.; Cosa, G. Chapter 1. Overview of Reactive Oxygen Species. In *Singlet Oxygen: Applications in Biosciences and Nanosciences*; Vol. *1*, Comprehensive Series in Photochemical & Photobiological Sciences; The Royal Society of Chemistry, 2016; pp. 1−21.
(66) Silhavy, T. J.; Kahne, D.; Walker, S. The Bacterial Cell Envelope. *Cold Spring Harbor Perspect. Biol.* **2010**, *2*, No. a000414.

(67) Alves, E.; Faustino, M. A.; Neves, M. G.; Cunha, A.; Tome, J.; Almeida, A. An Insight on Bacterial Cellular Targets of Photodynamic Inactivation. *Future Med. Chem.* **2014**, *6*, 141−164.
(68) Funes, M. D.; Caminos, D. A.; Alvarez, M. G.; Fungo, F.; Otero, L. A.; Durantini, E. N. Photodynamic Properties and Photoantimicrobial Action of Electrochemically Generated Porphyrin Polymeric Films. *Environ. Sci. Technol.* **2009**, *43*, 902−908.
(69) Gusev, I.; Ferreira, M.; Versace, D.-L.; Abbad-Andaloussi, S.; Pluczyk-Małek, S.; Erfurt, K.; Duda, A.; Data, P.; Blacha-Grzechnik, A. Electrochemically Deposited Zinc (Tetraamino)phthalocyanine as a Light-activated Antimicrobial Coating Effective against S. aureus. *Materials* **2022**, *15*, 975.
(70) Baigorria, E.; Durantini, J. E.; Martínez, S. R.; Milanesio, M. E.; Palacios, Y. B.; Durantini, A. M. Potentiation Effect of Iodine Species on the Antimicrobial Capability of Surfaces Coated with Electroactive Phthalocyanines. *ACS Appl. Bio Mater.* **2021**, *4*, 8559−8570.

https://doi.org/10.1021/acsapm.2c01890
ACS Appl. Polym. Mater. 2023, 5, 943−956